

Guest Editors: Sauro Pierucci, Jiří Jaromír Klemesš

Copyright © 2021, AIDIC Servizi S.r.l.
SBN 978-88-95608-84-6; ISSN 2283-9216

Development and techno-economic analysis of a two carriers reactor arrangement for chemical-looping combustion in a fixed bed

Claudio Tregambi, Piero Bareschino, Erasmo Mancusi*, Francesco Pepe

Dipartimento di Ingegneria, Università degli Studi del Sannio, Piazza Roma 21, 82100 Benevento, Italia

erasmo.mancusi@unisannio.it

Reduction of CO₂ emissions is imperative to stop climate change. In the present study, the performance of a system based on chemical looping combustion in fixed bed is investigated. The plant allows power generation with obtainment of a CO₂-rich stream ready for sequestration. To overcome the problems related to large temperature variations, use of two in-series oxygen carriers, Cu/CuO and Ni/NiO supported on Al₂O₃, is investigated. CH₄ was considered as fuel. A 1D numerical model was developed to estimate temperature and concentration profiles within the fixed bed as a function of time. A network of parallel reactors was designed to obtain continuous power generation at the turbine. A techno-economic analysis was performed to estimate plant throughput, overall efficiency, total capital costs, and levelized cost of energy of the proposed integrated plant.

Introduction

Carbon dioxide has been recognized as one of the main contributors to global warming. Carbon capture and sequestration technologies such as oxyfuel combustion, calcium looping and chemical looping combustion (CLC) may represent viable options to process conventional and/or renewable fuels in a clean way, allowing for production of concentrated CO₂ streams ready for subsequent sequestration (Adànez et al., 2012, Tregambi et al. 2020) or reutilization (Tregambi et al. 2021). CLC splits the conventional combustion in a two steps process. In the first stage, the fuel is reacted with a solid material which provides the O₂ required for the fuel oxidation. Since air is not fed, exhaust gas is not diluted with N₂ and a stream of pure CO₂ is produced upon water condensation. In the second step, the solid material is oxidized back with an air stream. Exhaust gas consists of O₂-lean air and can be released to the atmosphere upon heat recovery. The solid carrier usually consists of a metal oxide, referred as oxygen carrier (OC). First step of the process (fuel oxidation with OC reduction) can be endothermic or exothermic according to the fuel/OC couple, whereas the oxidation of the OC is always exothermic (Abad et al., 2007). Most of existing CLC reactors are based on two interconnected fluidized beds, one of them acting as the fuel-

reactor and the other one as the air-reactor (Diglio et al., 2017a). Alternatively, a packed bed reactor technology for CLC has been proposed (Noorman et al., 2007). In a packed bed, the OC particles are stationary and are alternately exposed to reducing and oxidizing conditions through a periodic switching of the feed conditions. The choice of the type of reactor and of the OC is crucial. Indeed, to achieve a high electricity efficiency the flue gas to be expanded in turbine needs to be produced at 20-30 bar and 1200 °C (Hamers et al., 2015). Fixed beds are more easily operated up to the high-pressure values required for subsequent gas turbine expansion of exhaust gas, and also reduce the problems of attrition/elutriation of the solid reactive material (Noorman et al., 2007). To circumvent the problem of maximum temperature achievable, Hamers et al. (2015) and Kooiman et al. (2015) proposed a two stage-CLC (TS-CLC) using the pair Cu/Mn in the first case and Cu/Ni in the second one. In both studies, syngas was used as fuel. An alternative option is represented by use of methane as fuel (Diglio et al., 2018). The aim of the present study is to investigate a CLC process in fixed bed reactors by exploiting the peculiarities of two-stage CLC, starting from material/energy balance toward techno-economic analysis. Methane was considered as fuel, whereas Cu/CuO and Ni/NiO were selected as active phase for the OCs. First, a transient model featuring heat and mass balance equations was developed to investigate the key performance of the system. Then, given the intrinsic intermittent nature of fixed beds, an integrated reactor network was designed with the aim of ensuring continuous power generation at the turbine. Finally, a techno economic analysis was performed to assess capital costs and levelized cost of energy.

Methodology

Mathematical model of chemical looping combustion

CLC process consists in a pressurized fixed bed with two in series OCs, a Cu-based OC in the first section, and a Ni-based OC in the second section. The reaction kinetic model for Cu/CuO (Abad et al., 2007) and Ni/NiO (Iliuta et al., 2010) carriers on γ -Al₂O₃ is summarized in Table 1.

Table 1: Kinetic scheme adopted

Reaction	ΔH_0 , kJ·mol ⁻¹	Reaction	ΔH_0 , kJ·mol ⁻¹
$2\text{Cu} + \text{O}_2 \rightarrow 2\text{CuO}$	-296	$\text{NiO} + \text{CO} \rightleftharpoons \text{Ni} + \text{CO}_2$	-43
$2\text{Ni} + \text{O}_2 \rightarrow 2\text{NiO}$	-479	$\text{NiO} + \text{CH}_4 \rightleftharpoons \text{Ni} + \text{CO} + 2\text{H}_2$	203
$4\text{CuO} + \text{CH}_4 \rightarrow 4\text{Cu} + \text{CO}_2 + 2\text{H}_2\text{O}$	-209	$\text{CH}_4 + \text{H}_2\text{O} \xrightleftharpoons{\text{Ni}} \text{CO} + 3\text{H}_2$	206
$2\text{NiO} + \text{CH}_4 \rightleftharpoons 2\text{Ni} + \text{CO}_2 + 2\text{H}_2$	161	$\text{CH}_4 + \text{CO}_2 \xrightleftharpoons{\text{Ni}} 2\text{CO} + 2\text{H}_2$	247
$\text{NiO} + \text{H}_2 \rightleftharpoons \text{Ni} + \text{H}_2\text{O}$	-2	$\text{CO} + \text{H}_2\text{O} \xrightleftharpoons{\text{Ni}} \text{CO}_2 + \text{H}_2$	-41

During oxidation stage (OS), air is fed and R₁ and R₂ occur in the first and second section of the reactor, respectively. Then, CH₄ is used to reduce CuO and NiO. During reduction stage (RS), the exothermic CuO reduction to Cu (R₃) occurs in the first section, while in the second section endothermic NiO reduction (R₄-R₇) occurs simultaneously to CH₄ reforming reactions (R₈-R₉). A detailed kinetic expression of reaction rate R₁ and R₃ can be found in Abad et al. (2007), while the

Ni oxidation (R_2) and reduction reaction rates are well presented by Iliuta et al. (2010). To describe axial concentration and temperature profiles in the reactor, a 1D pseudo-homogenous packed-bed model was used. The absence of radial concentration and temperature gradients, as well as the lack of both interphase and intra-particle concentration and temperature gradients has been validated and more details can be found in Mancusi et al. (2020). Governing equations for both OCs are reported in Table 2.

Table 2: Governing equations

Description	Equation
Gas phase mass balance	$\varepsilon_g \frac{\partial C_i}{\partial t} + u_g \frac{\partial C_i}{\partial z} = \varepsilon_g \frac{\partial}{\partial z} \left(D_{ax} \frac{\partial C_i}{\partial z} \right) + \varepsilon_g \rho_{oc} r_j$
Solid phase mass balance	$\frac{\partial X_k}{\partial t} = \frac{r_k}{C_{ok}}$
Energy balance	$[\varepsilon_g \rho_g c p_g + (1 - \varepsilon_g) \rho_s c p_s] \frac{\partial T}{\partial t} + (\varepsilon_g \rho_g c p_g u_g) \frac{\partial T}{\partial z} = \varepsilon_g \frac{\partial}{\partial z} \left(\lambda_{eff} \frac{\partial T}{\partial z} \right) + \varepsilon_g r_j (-\Delta H_j)$
Momentum balance	$-\frac{\partial P}{\partial z} = 150 \frac{\mu_g u_g (1 - \varepsilon_g)^2}{d_p^2 \varepsilon_g^3} + 1.75 \frac{\rho_g u_g^2 (1 - \varepsilon_g)}{d_p \varepsilon_g^3}$
Boundary conditions	$\frac{\partial C_i(0,t)}{\partial z} = \frac{u_g}{\varepsilon_g D_{ax}} (C_i(0,t) - C_{i,in}), \quad \frac{\partial C_i(L,t)}{\partial z} = 0$ $\frac{\partial T(0,t)}{\partial z} = \frac{u_g c p_g \rho_g}{\varepsilon_g \lambda_{eff}} (T(0,t) - T_{in}), \quad \frac{\partial T(L,t)}{\partial z} = 0$

In Table 2, the i index represents the gaseous species ($i=CH_4, H_2, CO_2, H_2O, CO, O_2, N_2$), while k ($k=Ni, Cu$) the solid carriers. The rates of formation or consumption of gas (r_j) and solid (r_k) species were calculated by summing up the reaction rates of those species in the reaction R_i in Table 1 for $i=1, \dots, 10$. C is the gas concentration in $\text{mol} \cdot \text{m}^{-3}$, C_{ok} is the initial concentration of solid species in the carrier, T is the temperature in K and X is the solid conversion, P is the pressure in Pa, z is the axial variable in m, t is the time in s, ε_g is the bed void fraction, u_g is the gas superficial velocity in $\text{m} \cdot \text{s}^{-1}$, D_{ax} is the axial dispersion in $\text{m}^2 \cdot \text{s}^{-1}$, ρ_{oc} and ρ_g are the density of oxygen carrier and gas, respectively, in $\text{kg} \cdot \text{m}^{-3}$, $c p_g$ is the gas heat capacity in $\text{J} \cdot \text{kg}^{-1} \cdot \text{K}^{-1}$, λ_{eff} is the effective thermal conductivity in $\text{W} \cdot \text{m}^{-1} \cdot \text{K}^{-1}$, d_p is the particle diameter in m, ΔH is the reaction enthalpy in $\text{kJ} \cdot \text{mol}^{-1}$. TS-CLC was modeled as two in-series fixed beds. Exit conditions of temperature and concentration from the first reactor represent the inlet to the second one. The infinite dimensional partial differential equations (PDEs) system has been reduced to a set of 400 ordinary differential equations (ODEs) by finite difference techniques which have been numerically solved by making use of the fortran library DLSODES (e.g. Altimari et al., 2012).

Design of the integrated system and techno economic analysis

Operation of the TS-CLC involves a sequence of five steps: i) oxidation stage (OS), where air is fed to the reactor for the OC oxidation; ii) heat removal (HR) step, during which air is fed to the reactor to extract the heat trapped by the OC as a consequence of the OS, and the resulting high-temperature gas stream is sent to turbine for expansion and power generation; iii) reduction

step (RS), during which the fuel is fed to the reactor to reduce the OC, completing the looping process. Two purge steps (PS) are required between stages ii) and iii) and after stage iii) to avoid formation of potentially explosive mixtures. In conclusion, the TS-CLC includes RS-PS-OS-HR-PS that cyclically follows each other in the fixed bed. During OS a stream of N₂ is produced which can be recycled in the HR step. During RS, a stream of CO₂ and H₂O is produced, which is sent to storage upon water condensation. To ensure continuous power generation at the turbine, a configuration of multiple in-parallel fixed beds needs to be designed, for which different approaches can be followed. Hamers et al. (2015) coupled CLC in fixed beds with an integrated gasification combined plant, meaning that a continuous stream of syngas needed to be processed. In this work, the fuel is CH₄ and it is considered to be available on demand. The reactor network was designed with the aim of obtaining a constant power production at the turbine, and with the two further goals of: i) keeping the investment costs as low as possible, and ii) avoiding the use of a gas buffer prior to the turbine. For this to occur, at least one reactor should always be within HR step, and it should be verified that:

$$\frac{\tau_{HR}}{\tau_{TOT}} \cdot N_r = 1 \quad (1)$$

where τ_{HR} is the duration of the HR step, τ_{TOT} the duration of a whole cycle, N_r the number of in-parallel reactors. Net power production (P_{net}) was estimated as difference between the power produced at the turbine and the sum of that required by the compressors and that possibly needed to preheat the reactants. Compression and expansion were modelled as single stage isentropic processes. An overall efficiency factor (η_{net}) was defined as:

$$\eta_{net} = \frac{P_{net} \tau_{TOT}}{W_{RS} LHV_{CH_4} \tau_{RS} N_r} \quad (2)$$

where W_{RS} is the stream of CH₄ fed during RS, LHV_{CH_4} the lower heating value of CH₄ and τ_{RS} the RS duration.

The reactor network was designed by accounting for the main components of the plant, namely: air/methane compressors, fixed bed reactors with OCs, high-temperature valves at reactor outlet for gas switching, turbine for power production. A sketch of the system is presented along with discussion of results, as a complete design is possible only upon solution of the mathematical model of CLC. Total capital costs (TCC) were then evaluated as sum of the individual costs of the different components. Costs of reactors and high temperature valves were computed according to Hamers et al. (2015), considering that fixed bed reactors embody an internal and external refractory, and a steel vessel. Cost of the individual materials was evaluated, and their sum multiplied by 4 to account for the reactor effective construction. OCs cost was estimated as sum of the individual metal oxides and inert support costs (Cu, Ni, γ -Al₂O₃), and again multiplied by 4 to account for the synthesis procedure. For turbine and compressors, equations from literature were used. Finally, levelized cost of energy was estimated as:

$$LCOE = \frac{TCC \cdot FCF + FOM}{8760 \cdot CF \cdot P_{net}} + VOM + \frac{SFC}{\eta_{net}} \quad (3)$$

where FCF is the fixed charge factor, computed considering 25 years of operation and a project interest ratio of 8.75%. Fixed operating and maintenance costs (FOM) were assumed to be 1% of the TCC and the capacity factor (CF) was set equal to 0.85. Variable operating and maintenance costs (VOM) were evaluated by considering replacement of OCs and of high temperature valves,

as well as the cost related to transport and storage of CO₂. Specific cost of the fuel (SFC) was considered.

Results and discussion

The core concept of TS-CLC is to transfer the heat developed during each stage in the first OC to the second one, so that the desired temperature increase can be gradually attained. The results of the numerical simulation of the TS-CLC are discussed below, and the parameters used are reported in Table 3.

Table 3: Model parameters used for TS-CLC numerical simulation

Parameter	Value	Parameter	Value	Parameter	Value
P_{in} , Pa	$20 \cdot 10^6$	L_{Cu} , m	1.0	w_{actNi}^0	0.11
$T_{in,OS}$, °C	450	L_{Ni} , m	1.0	w_{actCu}^0	0.14
$T_{in,RS}$, °C	550	d_r , m	0.7	m_{Cu} , kg	78.4
T_0 , °C	[450,950]	ε_g	0.6	m_{Ni} , kg	58
$\rho_g u_g _{OS/HR}$, kg·m ⁻² ·s ⁻¹	2	$\rho_g u_g _{RS}$, kg·m ⁻² ·s ⁻¹	2/15	$\rho_g u_g _{PS}$, kg·m ⁻² ·s ⁻¹	4

In Figure 1 are shown several spatial profiles during the main stages (RS, OS and HR) at the beginning and at the end of each stage. Since the Cu reduction reaction (R₂) is weakly exothermic while the Ni reduction stage is endothermic (R₄-R₉), in the first part of reactor the temperature increases, decreasing in the second one (see Figure 1a). The heat produced during RS in first reactor (Cu-based carrier) is then transferred to the second reactor, containing Ni-based carrier, to mitigate the temperature decrease due to the previous RS. Cu and Ni oxidation are both exothermic (R₁-R₂) and a sharp increase in the temperature is observed upon OS (Figure 1b). Once OS is completed the HR occurs and the heat produced during the previous OS is swept away and sent to the turbine. To power the turbine with an almost constant temperature HR is extended until outlet gas temperature drops below 1160 °C. More details about the control strategy that dictates the switch between each stage can be found in Mancusi et al. (2020) and Diglio et al. (2017b).

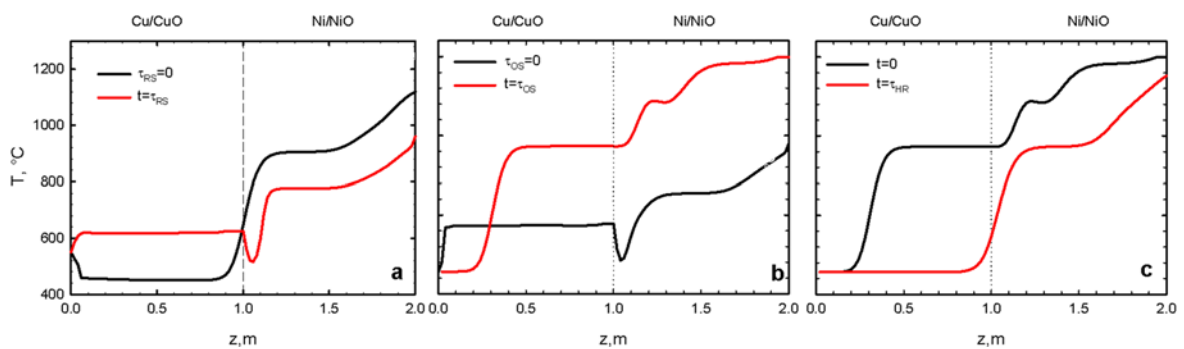


Figure 1: Spatial temperature profiles at several time instants during RS (a), OS (b) and HR (c)

Finally, in Figure 2 the outlet gas temperatures at the outlet of first and second reactor (a) and the O₂ and N₂ molar fractions (b) are reported for several CLC cycles when the regime conditions are attained.

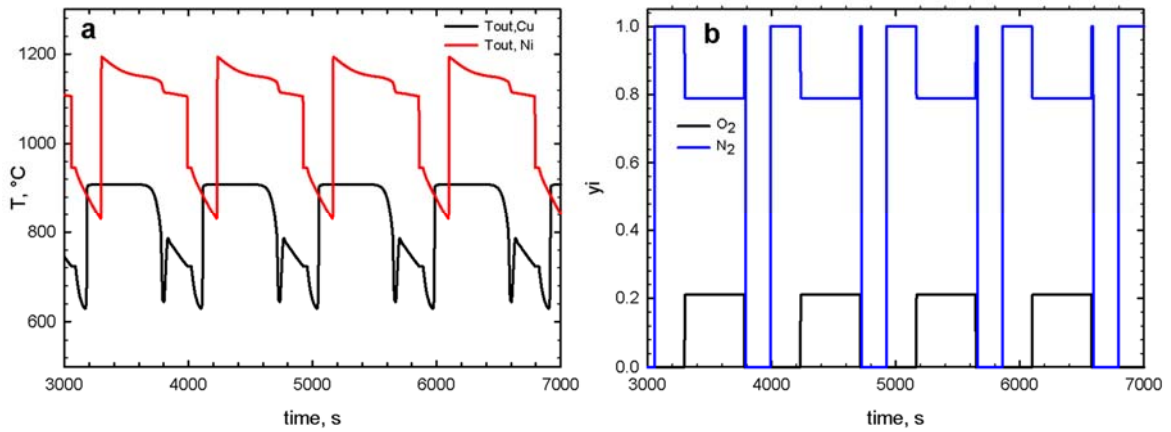


Figure 2: Outlet gas temperature (a) and N₂-O₂ concentrations (b) vs time for first and second OC.

It is possible to see that the temperature increase of 600 °C between inlet and outlet is equally split between the two oxygen carriers. The length of each stage was not fixed a priori, but a controller automatically sets it.

The time lengths found using the parameters set previously reported (see Table 3) are detailed in Table 4.

Table 4: Period of each stage

Stage	Oxidation	Purge	Reduction	Heat Removal	Purge	Overall
Value (s)	210	30	205	475	30	950

In order to produce a continuous hot gas stream to power the turbine, a system featuring in parallel reactors has to be operated. From Eq. (1) it is computed that N_r equals 2 for the investigated TS-CLC, as duration of the HR step equals half the overall cycle length. Therefore, an overall integrated scheme featuring two in parallel reactors was designed to attain a continuous power generation at the turbine. Figure 3 depicts the process scheme designed for the CLC operation. Only one of the reactors is sketched, the other working exactly in the same way but delayed in time. Thermal buffers, turbine, and compressors are shared between the two reactors.

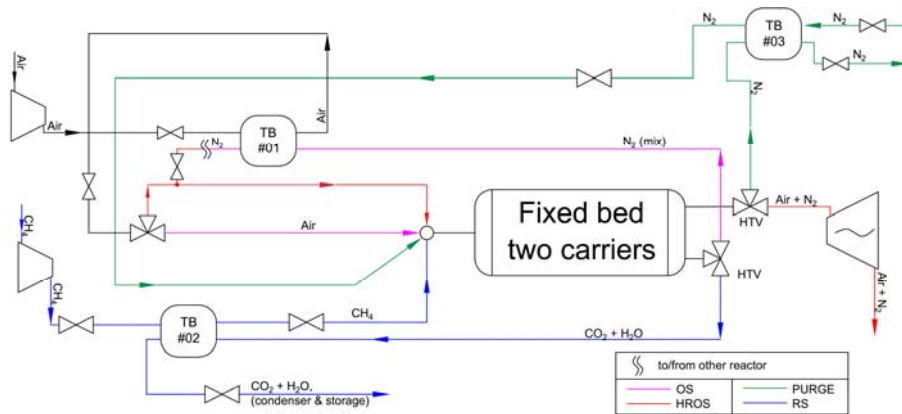


Figure 3: Sketch of the reactor network for the TS-CLC. HTV = high temperature valve, TB = thermal buffer

Preheating of the reactant streams can be performed by exploiting the sensible heat of the products streams, i.e. no auxiliary heat is required for the operation of the system and the whole power produced by the turbine can be sold to the market. More into detail, preheating of the air stream required for the OS and HR can be ensured by exploiting the sensible heat of the nitrogen stream exiting the OS. After heat recovery, the pressurized N_2 stream is recycled in the HR step to reduce power consumption of the compressor during the HR step. The same heat recovery strategy applies for preheating of the methane stream: sensible heat of the CO_2+H_2O stream produced after the reduction step can be recovered in a thermal buffer for the purpose. Finally, also for the PS the sensible heat of the impure N_2 exiting the system is used to preheat the stream of fresh N_2 .

Analysis of the power produced by the turbine and required by the compressors, not detailed here for the sake of brevity, disclose that the integrated reactor network can produce about 241 kW_e of energy, with an overall efficiency of 22%. Capital costs of the proposed integrated plant are instead detailed in Table 5.

Table 5: Total capital costs of the integrated plant

Component	High temperature valves	Reactors + oxygen carriers	Compressors	Turbine	Total
Cost (k€)	174.3	20.7	115.2	113.4	423.7

Total capital costs equal about 424 k€. The most expensive component are the high temperature valves required at the outlet of the fixed bed reactor, which account for about 41% of the TCC. Compressors and turbine account each for 27% of the total capital costs, whereas the fixed bed reactors and the oxygen carrier represent the smallest fraction of TCC, accounting for merely 5%.

Finally, levelized cost of energy is reported in Figure 4, split in the three main contributions related to: i) fuel; ii) variable operating and maintenance costs; iii) capital costs and fixed operating and maintenance costs.

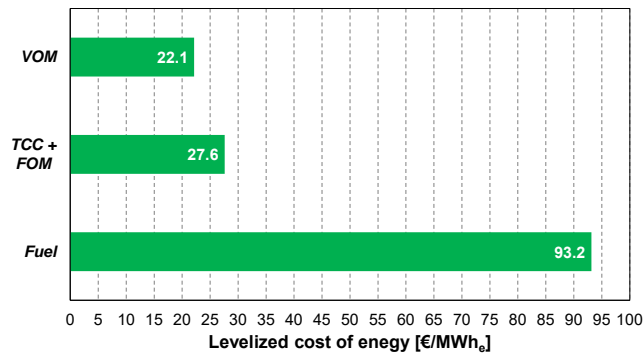


Figure 4: Levelized cost of energy for the TS-CLC, split in the three main contributions

The overall levelized cost of energy values about 134 €/MWh_e. This value is larger than that of conventional power plant or integrated gasification combined cycle based on coal or methane without carbon capture and storage, which generally ranges within 30–60 US\$/kWh_e. However, it harmonizes with data reported by other Authors for CLC in fixed beds (Mancuso et al., 2017). Main contribution to the levelized cost of energy arise from the price of the fuel and efficiency of the plant, responsible for about 65% of the total value of *LCOE*. A sensitivity analysis was performed by changing individually the cost of the different plant components. Fuel price is the main influencing variable, as a variation of $\pm 15\%$ in *SFC* induces a change in the *LCOE* of 10%. For the other components, when the cost changes within $\pm 15\%$, the effect on *LCOE* is below 1.5%.

Conclusion

The present study dealt with investigation of a two-stage chemical looping combustion process in fixed bed reactors and its related techno economic analysis. CH₄ was considered as fuel, and Cu/CuO followed by Ni/NiO as oxygen carriers. Model results indicate an outlet gas temperature of about 1200 °C during power production, with an increase equally split between the two metal oxides. Analysis of the system transient operation disclosed that at least two parallel reactors are required for continuous power production. The reactor network was designed, showing that preheating of the reactants can be fulfilled by recovering sensible heat of the products. An overall power production of about 240 kW_e was obtained, with an overall plant efficiency of about 22%. An investment of 424 k€ is estimated for the plant construction, mostly related to high temperature valves, compressors, and turbines. A levelized cost of energy of 134 €/MWh_e is foreseen, in agreement with other similar technologies of chemical looping combustion in fixed beds.

References

- Abad A., Adànez J., García-Labiano F., de Diego L.F., Gayà P., Celaya J., 2007, Mapping the range of operational conditions for Cu-, Fe-, and Ni-based oxygen carriers in chemical-looping combustion, *Chemical Engineering Science*, 62, 533–549.
- Adànez J., Abad A., García-Labiano F., Gayà P., de Diego L.F., 2012, Progress in Chemical-Looping Combustion and Reforming technologies, *Progress in Energy and Combustion Science*, 38, 215–282.
- Altimari P., Mancusi E., Russo L., Crescitelli S., 2012, Temperature wave-trains of periodically forced networks of catalytic reactors, *AIChE Journal*, 58, 899–913.

Diglio G., Bareschino P., Mancusi E., Pepe F., 2017a, Sensitivity analysis in the design of a packed-bed reactor for a chemical looping combustion process, *Chemical Engineering Transactions*, 57, 1027–1032.

Diglio G., Bareschino P., Solimene R., Mancusi E., Pepe F., Salatino P., 2017b, Numerical simulation of hydrogen production by chemical looping reforming in a dual fluidized bed reactor, *Powder Technology*, 316, 614–627.

Diglio G., Bareschino P., Mancusi E., Pepe F., 2018, Techno-Economic Evaluation of a small-scale power generation unit based on a Chemical Looping Combustion Process in Fixed Bed Reactor network, *Industrial & Engineering Chemistry Research*, 57, 11299–11311.

Garcia-Labiano F., de Diego L.F., Adànez J., Abad A., Gayà P., 2004, Reduction and oxidation kinetics of copper-based oxygen carrier prepared by impregnation for chemical-looping combustion, *Industrial & Engineering Chemistry Research*, 43, 8168–8177.

Hamers H.P., Romano M.C., Spallina V., Chiesa P., Gallucci F., van Sint Annaland M., 2015, Energy analysis of two stage packed-bed chemical looping combustion configurations for integrated gasification combined cycles, *Energy*, 85, 489–502.

Iliuta I., Tahoces R., Patience G., 2010, Chemical-looping combustion process: Kinetics and mathematical modeling, *AIChE Journal*, 56, 1063–1079.

Kooiman R. F., Hamers H.P., Gallucci F., Van Sint Annaland M., 2015, Experimental Demonstration of Two-Stage Packed Bed Chemical-Looping Combustion Using Syngas with $\text{CuO}/\text{Al}_2\text{O}_3$ and $\text{NiO}/\text{CaAl}_2\text{O}_4$ as Oxygen Carriers, *Industrial & Engineering Chemistry Research*, 54, 2001–2011.

Mancusi E., Bareschino P., Forgione A., Pepe F., 2020, A two carriers reactor configuration for chemical-looping combustion in a packed-bed, *International Journal of Greenhouse Gas Control*, 99, 103099.

Mancuso, L., Cloete, S., Chiesa, P., Amini, S., 2017, Economic assessment of packed bed chemical looping combustion and suitable benchmarks, *International Journal of Greenhouse Gas Control*, 64, 223–233.

Noorman S., van Sint Annaland M., Kuipers H., 2007, Packed Bed Reactor Technology for Chemical-Looping Combustion, *Industrial & Engineering Chemistry Research*, 46, 4212–4220.

Tregambi C., Di Lauro F., Montagnaro F., Salatino P., Solimene R., 2019, 110th Anniversary: Calcium Looping Coupled with Concentrated Solar Power for Carbon Capture and Thermochemical Energy Storage, *Industrial & Engineering Chemistry Research*, 58, 21262–21272.

Tregambi C., Bareschino P., Mancusi E., Pepe F., Montagnaro F., Solimene R., Salatino P., 2021, Modelling of a concentrated solar power – photovoltaics hybrid plant for carbon dioxide capture and utilization via calcium looping and methanation, *Energy Conversion and Management*, 230, 113792.